HEAT TRANSFER TO AN ISOTHERMAL FLAT PLATE IN TURBULENT FLOW OF A LIQUID OVER A WIDE RANGE OF PRANDTL AND REYNOLDS NUMBERS

A. Sh. Dorfman and O. D. Lipovetskaya

UDC 536.245:532.517.4

The study of heat transfer in turbulent flow over a flat plate is very important, not only because this situation frequently arises in practice, but also in that data for an isothermal flat plate are used to calculate heat transfer in more complex cases. In particular, such data are necessary when one uses the limiting relative laws which allow calculation of the effect of compressibility, pressure gradient, blowing, and other perturbing factors [1]. Most papers dealing with heat transfer for an isothermal flat plate refer to comparatively low Re values, when the velocity distribution in the boundary layer over almost its entire thickness can be described by the universal law of the wall. However, as Re increases there is an increasing layer adjacent to the outer boundary in which the velocity distribution cannot be described by the law of the wall, and therefore the results obtained for low Re are inapplicable. In the present paper coefficients of heat transfer from a turbulent flow to an isothermal flat plate have been obtained by numerical integration of the thermal boundary-layer equations over a wide range of the parameters $3 \cdot 10^5 \leq \mathrm{Re} \leq 2.5 \cdot 10^{12}$, $10^{-2} \leq \mathrm{Pr} \leq 10^3$.

Works [2-5] made use of equilibrium turbulent boundary layers characterized by a constant dimensionless pressure gradient $\beta = \delta^* \tau_w^{-1} dp/dx$. By integrating the dynamic layer equations Mellor and Gibson [5] calculated the velocity defect profiles for layers for various values of β, and in [6] this method of relating the velocity defect profiles with the universal law of the wall profiles was used, and a constituent function was proposed to determine the turbulent viscosity coefficient. Here the velocity and turbulent viscosity distributions in the layer were described by functions of the dimensionless coordinate $\eta = y/\Delta$, where $\Delta = \delta^*/\sqrt{c_f/2}$, depending on the parameters β and $\mathrm{Re}_* = \delta^* U/\nu$.

For these conditions and for a constant value of the turbulent Prandtl number Pr_t Dorfman [7] obtained solutions of the thermal boundary-layer equation for gradient equilibrium flows and arbitrary surface temperature distribution.

For the case considered here — an isothermal plate (T_w = const, $\beta = 0$) — these formulas have the form

$$\theta = (T - T_\infty)/(T_w - T_\infty) = G_0(\varphi), \quad \mathrm{St}(c_f/2\mathrm{Pr})q_0, \tag{1}$$

where $G_0(\varphi)$ is a function determined by integrating the ordinary differential equation given in [7]; $g_0 = -(2\beta_1/\mathrm{Re}_*)^{1/2}(\varphi^{1/2}G_0')_{\varphi=0}$; β_1 is a parameter depending on β and Re_* [5]; and φ is a variable uniquely related to the variable η [7],

$$\varphi = \beta_1 \sqrt{c_f/2} \int_0^\eta u/U d\eta. \tag{2}$$

In the calculations the turbulent Prandtl number Pr_t was assumed equal to unity. For large values of Prandtl number, when the thermal layer is located in the viscous sublayer, there is appreciable attenuation of fluctuations in the viscous sublayer. It is also assumed (e.g., in [8]), that the turbulent viscosity coefficient

Kiev. Translated from Zhurnal Prikladnoi Mekhaniki i Tekhnicheskoi Fiziki, No. 4, pp. 94-100, July-August, 1976. Original article submitted July 22, 1975.

This material is protected by copyright registered in the name of Plenum Publishing Corporation, 227 West 17th Street, New York, N.Y. 10011. No part of this publication may be reproduced, stored in a retrieval system, or transmitted, in any form or by any means, electronic, mechanical, photocopying, microfilming, recording or otherwise, without written permission of the publisher. A copy of this article is available from the publisher for $7.50.

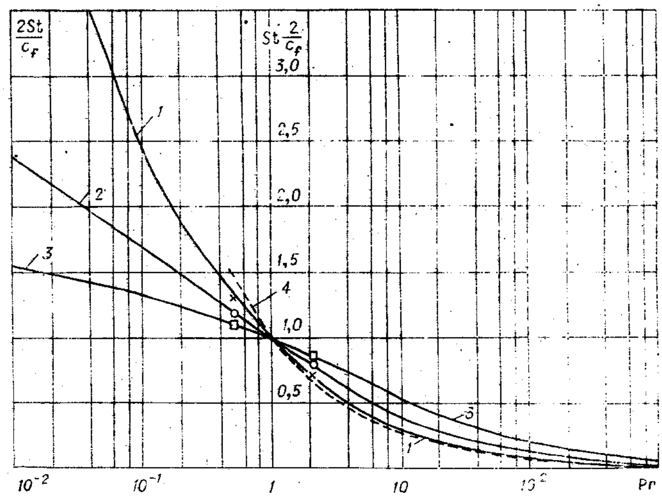

Fig. 1

is proportional to the fourth power of the distance from the wall. For $Pr < 1$, when the thermal layer is thicker than the dynamic layer, it is assumed that the turbulent viscosity coefficient does not vary outside the dynamic layer and is equal to its corresponding value at the outer edge of the dynamic layer [9].

Figure 1 shows results of calculations in the form of the Reynolds analogy coefficient $2St/c_f$ as a function of Prandtl number Pr, for various values of the parameter Re_* [for curve 1) $Re_* = 10^3$; 2) $Re_* = 10^5$; 3) $Re_* = 10^9$].

For comparatively low values of Re, and for values of Pr near unity, the results of the computations agree well with the formula $2St/c_f = Pr^{-0.6}$ (curve 4) and also with the value 1/0.863 (the point indicated by a triangle) obtained in [10] by reducing experimental data for air ($Pr = 0.7$).

The computations also agree well with results obtained for $Pr = 0.5$–2 and $1.2 \cdot 10^5 < Re_* < 1.11 \cdot 10^9$ in [11] by numerical integration of the system of turbulent boundary-layer differential equations, using the Clauser formula for the friction stress and the Cowles formula for the velocity distribution in the boundary layer (points of the curves 1–3).

For large values of Re the analogy coefficient values differ substantially from the corresponding values at low Re. The increase in Re leads to a growth for $Pr > 1$, and for $Pr < 1$ it leads to a reduction in the analogy coefficient.

In order to obtain an approximation for calculating the heat-transfer coefficients we use the following considerations. It was shown in [12] that for $Pr \to \infty$ the Stanton number is proportional to $\sqrt{c_f/2}$. In addition, it is well known that for $Pr = 1$ the Stanton number is proportional to $c_f/2$. From this we can predict that even for other Pr values there is a proportionality between St and $(c_f/2)^n$, and that the exponent decreases with increase of Prandtl number, from 1 at $Pr = 1$ to 0.5 for $Pr \to \infty$. From the relations given in Fig. 2 $\log St = f(\log c_f/2)$, obtained by calculation [for curve 1) $Pr = 1000$; 2) $Pr = 100$; 3) $Pr = 10$; 4) $Pr = 1$; 5) $Pr = 0.1$; 6) $Pr = 0.01$], it follows that this proportionality actually occurs for $Pr > 1$. Here the corresponding values of the exponent n are presented as a function of Prandtl number (curve 7). By replacing the curve $n = f(\log Pr)$ by two straight lines and determining the corresponding coefficients of proportionality between St and $c_f/2$, we obtain the approximations

$$St = Pr^{-1.35}(c_f/2)^{1-0.29 \lg Pr} \quad (1 < Pr \leqslant 50); \tag{3}$$

$$St = 0.113 Pr^{-3/4}(c_f/2)^{1/2} \quad (Pr > 50). \tag{4}$$

Figure 3 compares the results of the calculation using the last formula with experimental data of [12] [for curve 1) $Re_* = 10^3$; 2) $Re_* = 10^5$; 3) $Re_* = 10^9$]. The calculated curves $St\sqrt{2/c_f} = f(Pr)$, which merge into one curve for large Prandtl numbers, were continued into the region $Pr > 10^3$ by calculating the slope of the tangent at the point $Pr = 10^3$.

Good agreement is observed between the computed experimental data: the coefficient of proportionality is 0.113 in Eq. (4), as determined by calculation, and it practically coincides with the value 0.115 determined in [12] by comparison with experimental data. It can be seen from Fig. 3 that Eq. (4) describes the results

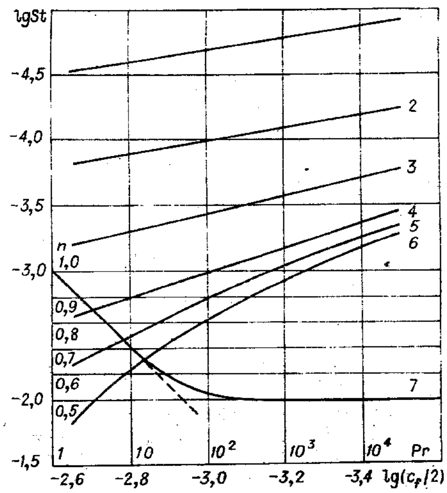

Fig. 2

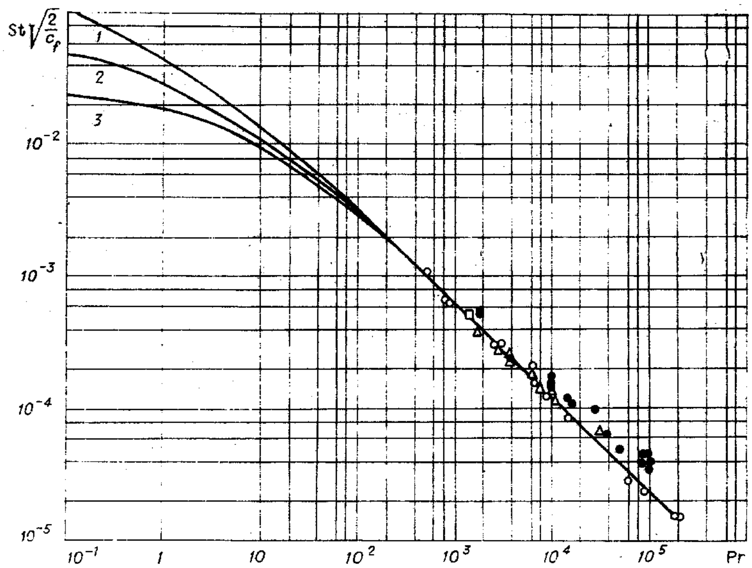

Fig. 3

obtained quite well for Pr > 50. For Pr < 50 the curves relating to different Re_* values diverge substantially, Eq. (4) is no longer appropriate, and in the region 1 < Pr < 50 the results are described by Eq. (3). The friction factor appearing in Eqs. (3) and (4) was determined from the equation

$$\sqrt{2/c_f} = (1/\varkappa)\ln \mathrm{Re}_* + 4.31, \tag{5}$$

where Re_* and Re_x are connected by the relation [7]

$$\mathrm{Re}_* = \beta_1 c_f/2 \cdot \mathrm{Re}_x. \tag{6}$$

These two equations connect c_f and Re_x implicitly. Therefore, for the calculations it is more convenient to use the Schlichting formula

$$c_f = (2\lg \mathrm{Re}_x - 0.65)^{-2.3},$$

which gives results close to those obtained using Eqs. (5) and (6).

From the data of Fig. 2 it can be seen that for Pr < 1 the results of the calculations cannot be approximated by functions of type (3) and (4): the dependence $\log(\mathrm{St}) = f(\log c_f/2)$ is nonlinear. However, it turns out

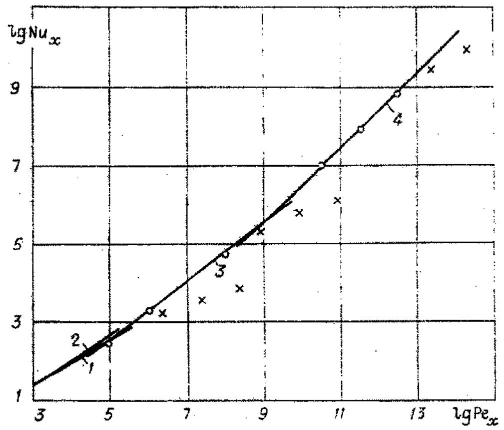

Fig. 4

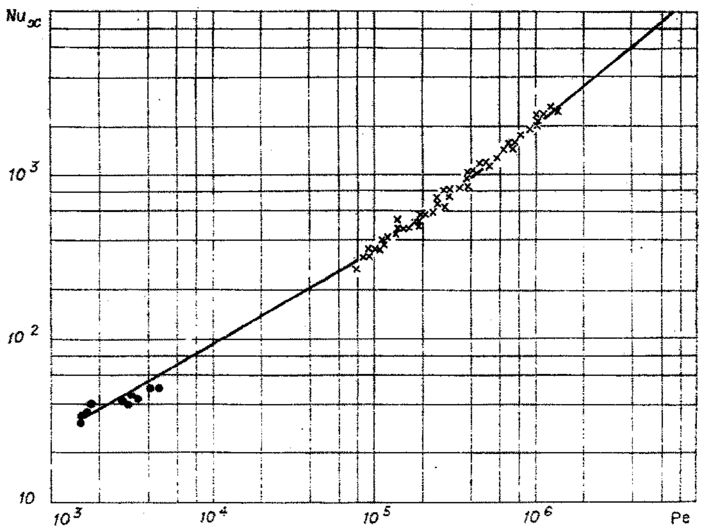

Fig. 5

that for Pr < 1 there is a unique relation $Nu_x = t(Pe_x)$ at all the Re values. This is given in Fig. 4, where the results obtained have been brought together on the graph $\log Nu_x = f(\log Pe_x)$, and it can be seen that all the points (denoted by circles) referring to the values Pr < 1 form a single curve, while the points (denoted by crosses) referring to values Pr > 1 do not fall on the curve.

In Fig. 5 the relation obtained $Nu_x = f(Pe_x)$ is compared with the results of experiments obtained in [13] for air (×) and in [14] for liquid metals (•). It can be seen that the theoretical results are in good agreement with the experimental data.

The unique relation $Nu_x = f(Pe_x)$ can be approximated by the formula

$$Nu_x^{-0.023} = 1.04 - 0.0335 \lg Pe_x,$$

analogous to the Schlichting formula for the friction factor. Simpler power relations can be obtained by approximating to this relation by several relations, for example, as in Fig. 4, by three straight lines.

The straight line 1 was constructed according to the equation

$$Nu_x = 0.282\, Pe_x^{0.62} \quad (10^3 < Pe_x < 10^5), \tag{7}$$

and the straight line 2 was constructed by the relation

$$Nu_x = 0.247 Pe_x^{0.65}, \tag{8}$$

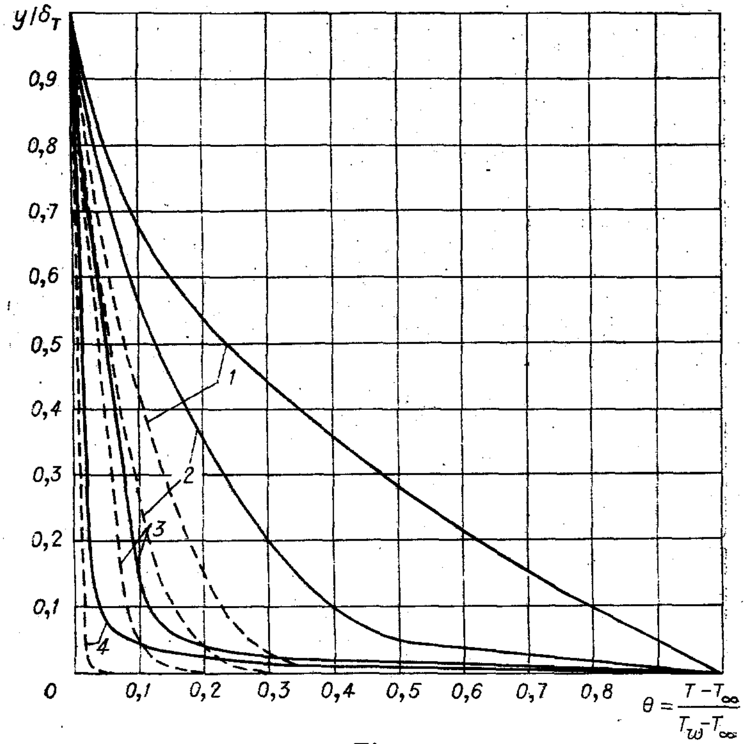

Fig. 6

obtained in [9] for $10^3 < Re_x < 2 \cdot 10^5$ and $0.005 < Pr < 0.05$ with a logarithmic velocity profile in the layer and a linear distribution of shear stress. It can be seen from Fig. 4 that with these values of Pe_x the results of our calculations and Eq. (7) are in good agreement with Eq. (8).

For large values of the Péclet number the results of the calculations can be approximated by two analogous relations (the straight lines 3 and 4 in Fig. 4):

$$Nu_x = 0.036\, Pe_x^{0.8} \quad (10^5 < Pe_x < 5 \cdot 10^8); \tag{9}$$

$$Nu_x = 0.00576\, Pe_x^{0.9} \quad (5 \cdot 10^8 < Pe_x < 2.5 \cdot 10^{12}). \tag{10}$$

The approximations (9) and (10) are suitable for $Pr < 1$ and give good results right up to $Pr = 1$ for large Re numbers ($Re_x > 10^7$).

The use of these formulas for low values of Re and Pr close to 1 leads to errors, which are 25% for $Re_x = 2 \cdot 10^5$ and $Pr = 1$. In this region of the parameters the well-known relations can be used.

Equations (3), (4), (7), (9), and (10) span practically the whole range of parameters encountered.

In conclusion in Fig. 6 we present the dimensionless temperature profiles $\theta(y/\delta_T)$ in the boundary layer, calculated using Eqs. (1) and (2) for various values of Pr and Re_* (the solid lines correspond to $Re_* = 10^3$ and the broken lines, to $Re_* = 10^9$; for curves 1, 2, 3, and 4 Pr has the values 10^{-2}, 1, 10, and 100). It follows from the data of Fig. 6 that the Reynolds number has an appreciable influence on the temperature distribution in the layer. This influence increases with decrease of Prandtl number and is qualitatively similar to the effect of Prandtl number.

LITERATURE CITED

1. S. S. Kutateladze and A. I. Leont'ev, Heat and Mass Transfer and Friction in the Turbulent Boundary Layer [in Russian], Énergiya, Moscow (1972).
2. F. Clauser, Problems of Mechanics [Russian translation], No. 2, Inostr. Lit., Moscow (1959).
3. A. A. Townsend, Structure of the Turbulent Shear Flow, Cambridge University Press.
4. I. K. Rotta, The Turbulent Boundary Layer [in Russian], Sudostroenie, Leningrad (1967).
5. D. L. Mellor and D. M. Gibson, Equilibrium Turbulent Boundary Layers [Russian translation], No. 2, Sb. Per. Mekhanika (1967).
6. D. L. Mellor, Effect of Pressure Gradient on Turbulent Flow near a Smooth Wall [Russian translation], No. 2, Sb. Per. Mekhanika (1967).

7. A. Sh. Dorfman, "Solution of the heat-transfer equation for equilibrium turbulent boundary layers with arbitrary temperature distribution on the wetted surface," Izv. Akad. Nauk SSSR, Mekh. Zhidk. Gaza, No. 5 (1972).
8. L. G. Loitsyanskii, "Heat transfer in turbulent flow," Prikl. Mat. Mekh., 24, No. 4 (1960).
9. S. S. Kutateladze, V. M. Borishanskii, I. I. Novikov, and O. S. Fedynskii, Liquid-Metal Heat-Transfer Agents [in Russian], Atomizdat, Moscow (1958).
10. S. W. Shi and D. B. Spalding, "Influence of temperature ratio on heat transfer to a flat plate through a turbulent boundary," in: Proceedings of the Third International Heat Transfer Conference, Vol. 11, New York (1966).
11. V. N. Popov, "Heat Transfer and drag in longitudinal turbulent flow of air over a flat plate," Teplofiz. Vys. Temp., 8, No. 5 (1970).
12. S. S. Kutateladze, Wall Turbulence, Part 1 [in Russian], Nauka, Novosibirsk (1970).
13. B. S. Petukhov, A. A. Detlof, and V. V. Kirillov," Experimental investigation of local heat transfer to a flat plate in subsonic turbulent air flow," Zh. Tekh. Fiz., 24, No. 10 (1954).
14. E. D. Fedorovich, "Heat transfer to a flat plate washed by a turbulent boundary layer," Inzh.-Fiz. Zh., No. 9 (1959).

EFFICIENCY OF A THERMAL CURTAIN

E. V. Shishov

UDC 532.517.4

Gas curtains are widely used to protect surfaces washed by a high-enthalpy gas flow.

The main parameter describing the heat transfer under these conditions is the curtain efficiency

$$\theta = \frac{T_W^* - T_0}{T_{W_1} - T_0} = \frac{\delta_{T_1}^{**}}{\delta_{T_{ad}}^{**}},$$

where T_0 is the temperature of the unperturbed stream; T_W^* is the adiabatic wall temperature; T_{W_1} is the wall temperature at the curtain entrance point; $\delta_{T_{ad}}^{**}$ is the energy loss thickness on the adiabatic wall; and $\delta_{T_1}^{**}$ is the energy loss thickness at the curtain entrance point.

Several authors [1-3] have proposed analytical expressions to determine the efficiency of the thermal curtain; in [2, 3] these expressions were given for the limiting case $x \to \infty$.

However, in a number of cases of practical engineering importance the length of the protected surfaces is small, and there is therefore a need for more accurate determination of thermal curtain efficiency in the entrance section. An analytical expression for this case can be obtained from the following assumptions. It is well known [1, 2] that under these conditions the law of superposition of thermal fields is applicable, and one can therefore assume that a new thermal perturbation resulting from the effect of the wall being adiabatic will grow in the existing thermal boundary layer in the same way as the thermal boundary layer grows under the conditions of the preceding adiabatic section.

Figure 1 shows the temperature profile on an adiabatic wall (solid line). In order to show how a new thermal perturbation develops, i.e., the region with zero temperature gradient, it is convenient to represent the dimensionless temperature in the form

$$(T_{W_1} - T)/(T_{W_1} - T_0).$$

Moscow. Translated from Zhurnal Prikladnoi Mekhaniki i Tekhnicheskoi Fiziki, No. 4, pp. 100-103, July-August, 1976. Original article submitted July 22, 1975.

This material is protected by copyright registered in the name of Plenum Publishing Corporation, 227 West 17th Street, New York, N.Y. 10011. No part of this publication may be reproduced, stored in a retrieval system, or transmitted, in any form or by any means, electronic, mechanical, photocopying, microfilming, recording or otherwise, without written permission of the publisher. A copy of this article is available from the publisher for $7.50.